Properties of tantalum oxynitride thin films produced by magnetron sputtering: The influence of processing parameters

D. Cristea, D. Constantin, A. Crisan, C.S. Abreu, J.R. Gomes, N.P. Barradas, E. Alves, C. Moura, F. Vaz, L. Cunha

A B S T R A C T

The main purpose of this work is to present and to interpret the change of structure and physical properties of tantalum oxynitride (TaN_xO_y) thin films, produced by dc reactive magnetron sputtering, by varying the processing parameters. A set of TaN_xO_y films was prepared by varying the reactive gases flow rate, using a N_2/O_2 gas mixture with a concentration ratio of 17:3. The different films, obtained by this process, exhibited significant differences. The obtained composition and the interpretation of X-ray diffraction results, shows that, depending on the partial pressure of the reactive gases, the films are: essentially dark grey metallic, when the atomic ratio $(N + O)/Ta < 0.1$, evidencing a tetragonal β-Ta structure; grey-brownish, when $0.1 < (N + O)/Ta < 1$, exhibiting a face-centred cubic (fcc) TaN-like structure; and transparent oxide-type, when $(N + O)/Ta > 1$, evidencing the existence of Ta_2O_5, but with an amorphous structure. These transparent films exhibit refractive indexes, in the visible region, always higher than 2.0.

The wear resistance of the films is relatively good. The best behaviour was obtained for the films with $(N + O)/Ta \approx 0.5$ and $(N + O)/Ta \approx 1.3$.

Keywords:
Tantalum oxynitride
Structure
Optical properties
Tribological behaviour

1. Introduction

Transitional metal oxynitrides are a new class of materials with properties that could be implemented in industrial applications. The main advantage of such coatings is the possibility to tune their chemical, mechanical, electrical and optical properties to suit the desired application. By varying the ratio between the nitrogen and oxygen, one could obtain properties ranging from nitride-like hard, metallic and chemically inert coatings to oxide-like electrically insulating coatings, suited for dielectric, optical or decorative applications [1–8]. Tantalum oxynitride can benefit from the properties exhibited by tantalum nitride, which is known to be used as a hard and refractory material for tribological and mechanical purposes [9], for electrical applications as either a conductive or insulating material [10–12] and also from optical, dielectric and decorative properties of the tantalum oxide [13–15], as well as for its biomedical potential applications [16,17]. Thus, tuning the nitrogen/oxygen ratio may lead to potentially attractive properties. This paper presents the findings related to the chemical and structural evolution as a function of the reactive DC sputtering deposition parameters and the influence of such parameters on the composition, structure and on the optical and tribological behaviour of tantalum oxynitride thin solid films.

2. Experimental details

For the present work, TaO_xN_y thin films were deposited onto glass, silicon (100), high-speed steel (AISI M2) and stainless steel (AISI 316) substrates, by DC reactive magnetron sputtering, using a laboratory-size deposition chamber. The configuration of the deposition system is two unbalanced type II magnetrons with a rectangular shape, facing each other. For this study only one of the magnetrons was used, in a closed field configuration. A dc current density of 50 A/m^2 was used during all depositions. The tantalum

target dimensions are (200 × 100 × 6) mm and its purity is 99.6%. The films were obtained in a rotation mode, to improve their homogeneity, and the substrate holder was positioned at a distance of 70 mm, in front of the target, during all runs. All the samples were produced with grounded substrates. Before each deposition, the substrates were plasma-etched during 500 s, using a pulsed current of approximately 0.6 A in a pure argon atmosphere with a partial pressure around 0.3 Pa. During depositions the atmosphere inside the chamber was composed of a mixture of Ar + N_2 + O_2. An argon flow of 60 sccm was kept constant during all depositions, while the 85% N_2 + 15% O_2 gas mixture (17/3 concentration ratio) was varied between 2.5 and 30 sccm. For comparison purposes one of the samples was deposited without the presence of reactive gases. The working pressure varied between 0.4 Pa and 0.65 Pa, depending on the flow rate of the reactive gas mixture. The substrate holder was maintained at a temperature of 100 °C.

The atomic composition was measured by Rutherford Backscattering Spectrometry (RBS) using protons with energy of 2.25 MeV, at an angle of incidence of 0° and with three detectors in the chamber: standard at 140°, and two pin-diode detectors located symmetrically to each other, at 165°. The resulting profiles were generated using the IBA DataFurnace NDF software program [18]. X-ray diffraction investigations were performed on Si substrates samples using a Philips PW diffractometer (Cu-Kα radiation) in a Bragg-Brentano geometry configuration. The resulting patterns were processed with a Pearson VII function in order to obtain the peak characteristics: position, intensity and full width at half maximum (FWHM).

The reflectance and transmittance were measured on a UV–Vis–NIR spectrophotometer (Shimadzu UV–Vis–NIR 2505) in the spectral range of 250–800 nm.

Film colour was determined from the reflectance spectra obtained in the wavelength range 400–700 nm, using a Minolta (Cm-2600d) portable spectrophotometer. The colour was represented by the parameters L*, a*, b*, according the CIELAB 1976 colour space. In this three coordinate system, L* represents the lightness which varies from 0 (black) to 100 (diffuse white), taking into account that specular white is evidence of higher values. The chromaticity coordinates are a* and b*: a* varies from green (negative values) to red/magenta (positive values); and b*varies from blue (negative values) to yellow (positive values). In the case of chromaticity coordinates, the farther from (0,0), the higher the colour saturation.

The thickness of the films was obtained by ball-cratering, while residual stress values were calculated with Stoney's equation [19], using the curvature radii of the stainless steel samples before and after the film depositions. The tribological characterization of the high speed steel coated samples was carried out on a reciprocating tribometer, under ambient conditions, using silicon nitride balls with 5 mm diameter as a counterpart material, and a constant normal applied load of 0.5 N. In all tests, the track length and the frequency of the oscillating motion of the plate were kept constant at values of 6 mm and 1 Hz, respectively.

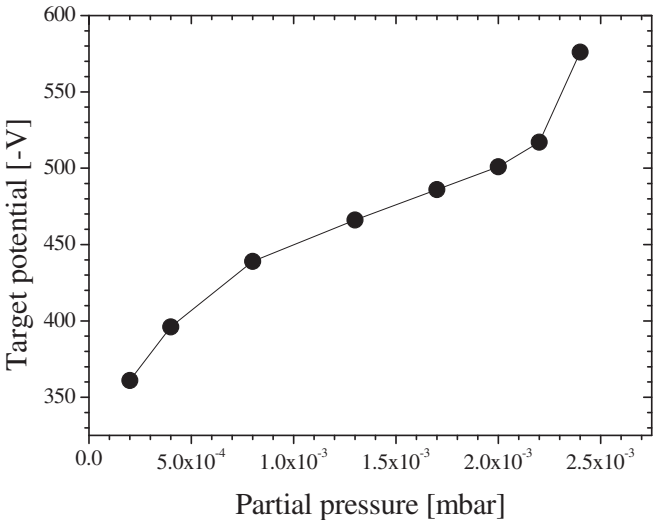

Fig. 1. Target potential as a function of the partial pressure of the reactive gases.

3. Results and discussion

3.1. Deposition rate and film composition

In Table 1 are registered the different deposition conditions and some characteristics of the deposited tantalum oxynitride films.

The registered partial pressure of the reactive gases was measured before the discharge ignition. The films revealed low values of residual stress, less than 1 GPa and compressive in nature. Only in the case of the sample $TaN_{0.55}O_{0.45}$, a small tensile stress (∼270 MPa) was detected.

Fig. 1 shows the evolution of the target potential as a function of the partial pressure of the reactive gas mixture. As is readily seen, an increase of the partial pressure results in an increase of the target potential. This may be due to the increase in the overall reactive gas flow, which enhances the target poisoning effect.

The influence of the partial pressure of the reactive gases on the deposition rate can be observed in Fig. 2. The deposition rate does not vary significantly with the increase of the partial pressure (between ∼18 nm/min and ∼22 nm/min). Nevertheless a pattern seems to emerge. There can be seen a gradual increase in the deposition rate up to a partial pressure of the of reactive gas mixture of 1.7×10^{-3} mbar, followed by a gradual decrease. This decrease may be explained by the target poisoning effect and by the structural evolution of the samples. As will be shown in the structural evolution discussion, between 1.7×10^{-3} mbar and 2.0×10^{-3} mbar, a change from the possibly nitride-like structure to a more oxide-oriented structure occurs. The higher reactivity of the oxygen might lead to an increase above the maximum gettering capacity of the reactive gas, which translates in a higher quantity of

Table 1
Characteristics and different deposition conditions of the produced TaN_xO_y films: Φ (N_2 + O_2) – reactive gases flow; P (N_2 + O_2) – reactive gases partial pressure; t_f, films' thickness; σ – residual stress.

Samples	Atomic ratio (N + O)/Ta	Φ (N_2 + O_2) [sccm]	P (N_2 + O_2) [mbar]	t_f [μm]	σ [GPa]
Ta N_0O_0	0	0.0	0	1.42 ± 0.07	–
$TaN_{0.07}O_{0.03}$	0.10	2.5	2.0×10^{-4}	1.15 ± 0.10	−0.30 ± 0.05
$TaN_{0.27}O_{0.20}$	0.47	5.0	4.0×10^{-4}	1.26 ± 0.07	−0.75 ± 0.10
$TaN_{0.55}O_{0.45}$	1.00	10.0	8.0×10^{-4}	1.30 ± 0.08	+0.27 ± 0.11
$TaN_{0.54}O_{0.49}$	1.03	15.0	1.3×10^{-3}	1.34 ± 0.09	−0.64 ± 0.08
$TaN_{0.47}O_{0.67}$	1.14	20.0	1.7×10^{-3}	1.37 ± 0.08	−0.91 ± 0.11
$TaN_{0.41}O_{0.91}$	1.32	22.5	2.0×10^{-3}	1.31 ± 0.10	−0.11 ± 0.09
$TaN_{0.39}O_{0.91}$	1.30	25.0	2.2×10^{-3}	1.21 ± 0.04	−0.05 ± 0.03
$TaN_{0.32}O_{1.24}$	1.56	30.0	2.4×10^{-3}	1.13 ± 0.08	−0.26 ± 0.12

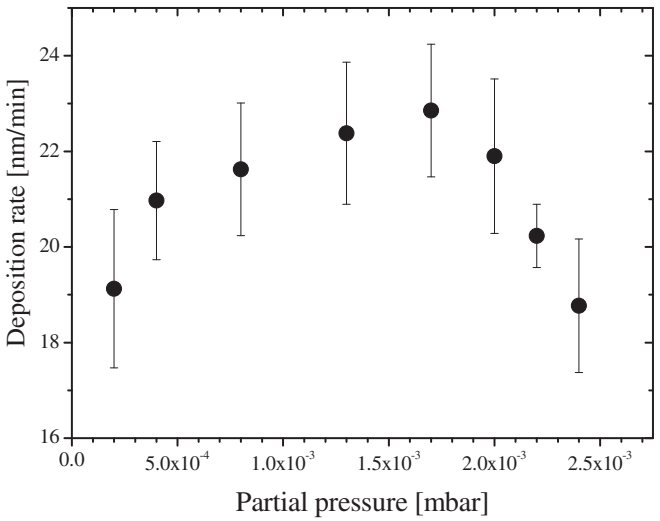

Fig. 2. Deposition rate as a function of partial pressure of reactive gases. Error bars were determined by the maximum deviation to the average value.

compound inside the deposition chamber, and subsequently on the target. Simulations and modelling of the reactive sputtering deposition processes using two reactive gases have shown that the deposition process response is unlike that one found when only one reactive gas is used [20]. Both reactive gases compete during compound formation, both on the target and on the substrate, which implies that both reactive gases contribute to the target poisoning effect. Usually the sputtering yield of both compounds (oxide and nitride) is lower than that of the metallic target, affecting the deposition rate and partial pressure inside the chamber. In this case, it seems that a stronger influence of oxygen than that one of the nitrogen occurs, above 1.7×10^{-3} mbar of reactive gas partial pressure, leading to a decrease in the deposition rate.

For a better understanding of the correlation between the deposition parameters and their effect on the structural change and, subsequently, on the properties exhibited by them, the chemical composition was analyzed and the results are plotted in Fig. 3a, as a function of partial pressure of the reactive gases. About these results it is important to notice that the tantalum RBS signal is large and isolated, and the error in its concentration is around 2 at.%. The nitrogen and oxygen RBS signals are smaller, superimposed to the Si substrate signal and to each other and, therefore, the error in their concentration is larger, up to 5 at.%. The non-metal/metal atomic ratios are also represented (Fig. 3b). As expected, when the partial pressure of the reactive gases increases, O and N concentrations tend to increase, while the Ta concentration decreases. However, there exist details that worth mentioning. It is important to note that in all the films produced with reactive gases partial pressure equal or lower than 1.3×10^{-3} mbar, the N/Ta ratio exceeds the O/Ta ratio. For these films, the difference between the N/Ta and O/Ta ratios is small but, as will be seen in the structural and properties analysis, they exhibit a dominant metallic or nitride-like behaviour. Above 1.3×10^{-3} mbar, an inversion occurs, with the O/Ta ratio becoming increasingly higher than the N/Ta ratio, resulting in the prevalence of an oxide-like behaviour of the films. The complete set of produced samples may be divided into 4 different compositional zones:

Zone 1 ($p(N_2 + O_2) < 2 \times 10^{-4}$ mbar): films exhibiting a non-metal to tantalum atomic ratio equal or lower than 0.10. The films might be considered as tantalum, containing a certain amount of oxygen and nitrogen, depending of the partial pressure of reactive gases;

Zone 2 (2×10^{-4} mbar $< p(N_2 + O_2) < 8 \times 10^{-4}$ mbar): films exhibiting a non-metal to tantalum atomic ratio lower than one. The increase of the partial pressure causes a constant increase of the oxygen and nitrogen content;

Zone T (8×10^{-4} mbar $< p(N_2 + O_2) < 1.3 \times 10^{-3}$ mbar): films exhibiting a stabilization of the non-metal to metal atomic ratio (close, but slightly higher than one). They exhibit a slight increase of O content and a slight decrease of the N content when the partial pressure increases. This zone gets its name, *transition zone*, because of its location in-between the nitride-like films, produced with lower partial pressures (zone 2), and the oxide-like films (zone 3);

Zone 3 ($p(N_2 + O_2) > 1.3 \times 10^{-3}$ mbar): films exhibiting a non-metal to tantalum ratio increasing progressively up to ~1.6. A particular feature of this zone is the consistent decrease of N concentration, as opposed to an increase of O concentration. The sample produced with a partial pressure of 1.7×10^{-3} mbar, $TaN_{0.47}O_{0.67}$, might be considered the starting point of the oxide-like behaviour. The partial pressure of O_2 in the deposition chamber is significantly lower than that of N_2. Nonetheless, in this zone, the oxygen content in the films is higher than that of the nitrogen, which indicates that the film's formation is thermodynamically driven. As a matter of fact, when comparing N and O content of the films, all of them exhibit a significantly higher O content than could be inferred strictly from the composition of the reactive atmosphere. The O/N ratio of the atmosphere in the deposition chamber

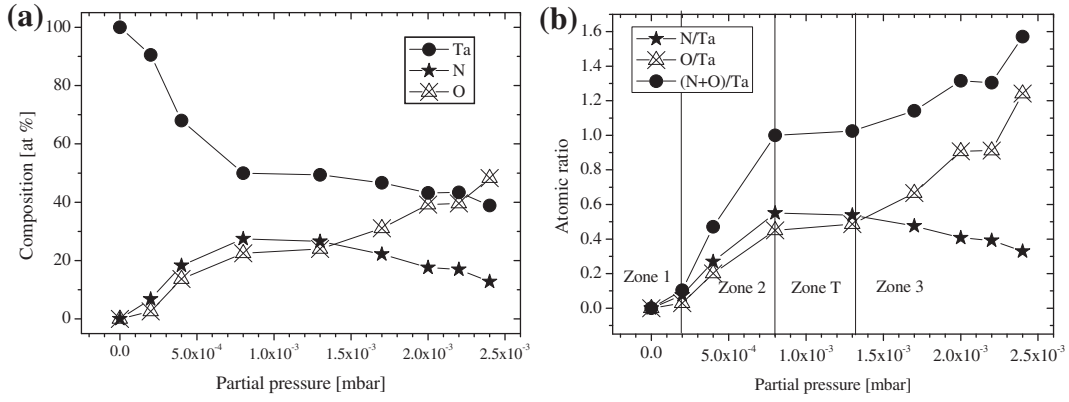

Fig. 3. Evolution of the chemical composition (a) and atomic ratios (b) as a function of the reactive gas mixture partial pressure. The partial pressure was measured before the discharge ignition. The error of the chemical composition is around 2 at.% for Ta and lower than 5 at.% for O and N.

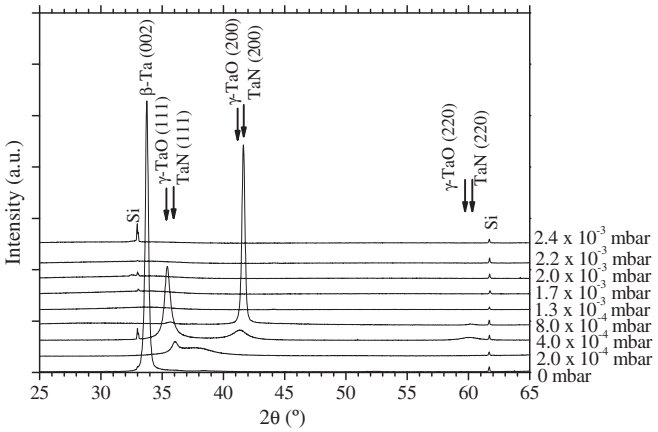

Fig. 4. X-ray diffraction patterns of the TaN_xO_y films as function of the reactive gases partial pressure. The peaks marked with "Si" correspond to the silicon substrate.

is always 0.176, while the smallest O/N ratio in the produced oxynitride films is 0.382. It seems that the affinity of tantalum toward oxygen is higher than the one towards nitrogen. The enthalpy of formation of tantalum nitrides and oxides helps to understand this behaviour. Values of the enthalpy of formation found in the literature for TaN, TaO, TaO_2 and Ta_2O_5 are −251 kJ/mol [21], 232 kJ/mol [22], −201 kJ/mol [21,22] and −2046 kJ/mol [21,22], respectively. Excepting the case of TaO, all the other processes are exothermic, being the Ta_2O_5 phase, and to lesser extent the TaN phase, those who exhibit the highest values of enthalpy of formation. Such values may account for the properties of nitride-like (for $p(N_2 + O_2) < 1.3 \times 10^{-3}$ mbar) and oxide-like (for $p(N_2 + O_2) > 1.3 \times 10^{-3}$ mbar) samples. For the highest partial pressures, when the oxygen partial pressure in the chamber atmosphere is enough to promote essentially the production of the Ta_2O_5 phase, this pentoxide becomes the dominant compound of the films and, as will be seen, they are essentially amorphous. When the oxygen partial pressure is not enough, the formation of the TaN phase is promoted, and the films may reveal the presence of crystalline fcc TaN. Nevertheless, looking at the atomic composition, the lattice may have oxygen atoms substituting some of the N atoms in the TaN structure. The discussion concerning the structural characterization will probably contribute to a better understanding of the phenomena behind the growth of these types of films.

3.2. Structural characterization

From the obtained XRD patterns (Fig. 4), a correlation between the structure and the compositional zones referred to in the previous section can be established. The coating deposited without reactive gases in the chamber, $Ta\,N_0O_0$, reveals the tetragonal phase (P42/mnm (136)) of Tantalum (β-Ta) (00-025-1280), strongly oriented with the (002) direction and slightly shifted to a higher diffraction angle. The size of the crystallites, measured from this peak, was 29 nm.

The film produced with a reactive gas partial pressure of 2×10^{-4} mbar seems to reveal the structure of tetragonal phase β-Ta as well, but with a higher degree of amorphization. A broad peak ranging from ∼36.6° to ∼41.3° exists, which is characterized by the location of several peaks of the β-Ta structure. The peak located at 36.03° may be assigned to the (410) plane of β-Ta. The maximum of the broad peak occurs at ∼38.03° and the (202) peak of β-Ta is located at 38.201°. The shift is similar to the one of the (410) plane (around 0.2°). The higher degree of amorphization of this film is probably due to the existence of O and N atoms, which may be incorporated in tantalum crystals.

The XRD patterns of the samples belonging to the compositional zone 2 ($TaN_{0.27}O_{0.20}$ and $TaN_{0.55}O_{0.45}$) reveal three diffraction peaks, located close to the angular positions of the unconstrained diffraction peaks of the (111), (200) and (220) planes of the face centred cubic (fcc) phase (Fm-3m (225)) of TaN (00-049-1283) or to the fcc phase of tantalum oxide (γ-TaO) (03-065-6750). Assuming this structure, the average lattice parameter of the crystallites, calculated from the three diffraction peaks of the samples, are 0.43679 nm, for the $TaN_{0.27}O_{0.20}$ sample, and 0.43452 nm, for the $TaN_{0.55}O_{0.45}$ sample. The lattice parameter of unconstrained fcc TaN and γ-TaO crystals is 0.43399 nm and 0.4380 nm, respectively. Therefore, the magnitude of the lattice parameter of the crystallites detected in zone 2, is inside these two limits, which seems to indicate that, probably, fcc Ta(N,O) crystallites are present in the films. This would correspond to a structure with O atoms substituting some of the N atoms of the fcc TaN structure and/or N atoms substituting O atoms of the γ-TaO structure. The peaks of the sample deposited with a higher partial pressure are broader and less intense. The broadness indicates a tendency to disorganized and smaller crystals, probably due to a higher amount of N or O substitutions in the crystallites. It is also important to notice that in the films of zone 2, a change in the preferential growth direction, from (111) of the film produced with lower partial pressure to (200) for the one produced with higher partial pressure is detected.

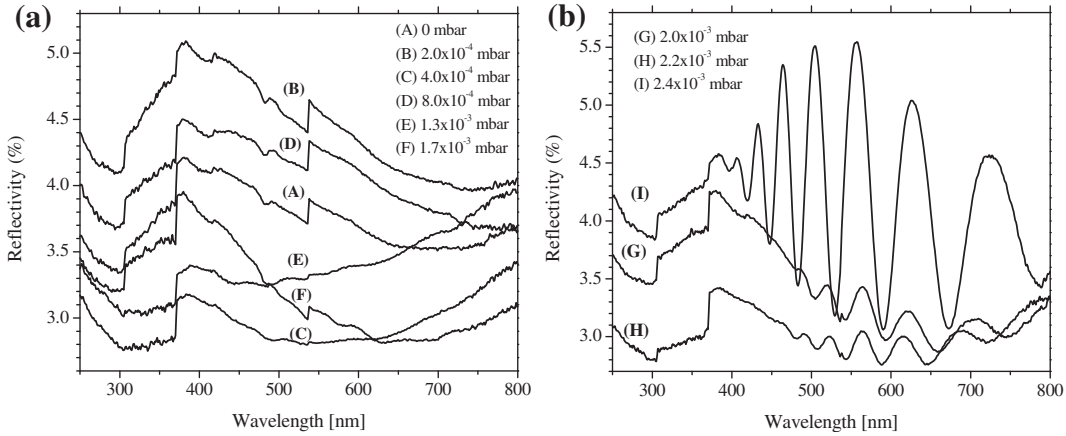

Fig. 5. Reflectivity as a function of wavelength of the TaN_xO_y films for several reactive gas partial pressures: (a) coatings produced with partial pressure below 2×10^{-3} mbar; (b) coatings produced with partial pressure above or equal to 2×10^{-3} mbar.

This change of preferential orientation, from (111) to (200) direction was also reported previously in the zirconium oxynitride system [23]. Measured grain size values of 12 nm for the $TaN_{0.27}O_{0.20}$ sample, obtained from the (111) peak, and of 39 nm for the $TaN_{0.55}O_{0.45}$ sample, obtained from the (200) peak, were assessed in the present work.

For higher partial pressures, with the corresponding increase of O content and reduction of N content, films belonging to compositional zone 3 reveal themselves as essentially amorphous. Moreover, a broad and low intensity peak, ranging from $2\theta \approx 24°$ to $2\theta \approx 37°$, is detected. Its location coincides with the location of several peaks of the body centred orthogonal structure (Ibam (72)) of tantalum oxide (Ta_2O_5) (00-054-0432).

3.3. Optical characterization

The samples were analyzed concerning their optical properties, by reflectance and transmittance spectroscopy. Fig. 5 represents the reflectivity of the tantalum oxynitride films as a function of the wavelength of the incident radiation. It can be observed that, for partial pressures below 2×10^{-3} mbar (Fig. 5a), the reflectance spectra of the films exhibit a significantly different behaviour when compared to those of compositional zone 3 (Fig. 5b). This set of samples exhibit an interference-like behaviour due to their transparency to visible radiation, which is an evidence of the presence of tantalum oxide, Ta_2O_5. For the samples that do not show interference-like behaviour (Fig. 5a) it can be observed that, in general, the reflectivity of all these films is low (lower than 5%) and a systematic variation of the reflectivity as function of the partial pressure of the reactive gases is not detected. In any case the difference of the reflectivity, among this set of samples, is not significant.

As is well known, the shape of the reflectivity curve of each spectrum depends on the particular composition of each film, as well as on the wavelength range, but basically, the registered behaviour is coherent with the decrease of the metallic characteristics of the films when the non-metal content increases.

Additional transmittance spectra were obtained for the samples that exhibit interference-like behaviour. This analysis was performed on samples deposited onto glass substrates. The results are plotted in Fig. 6a. For comparison reasons the transmittance spectrum of the sample produced with 1.7×10^{-3} mbar, $TaN_{0.47}O_{0.67}$, is also depicted. The composition of this film is the closest to the first composition that exhibits interference-like behaviour, being also the sample that first reveals an O content higher than N content, and helps to understand the gradual transition from metallic-like, opaque behaviour, to the oxide-like, transparent behaviour.

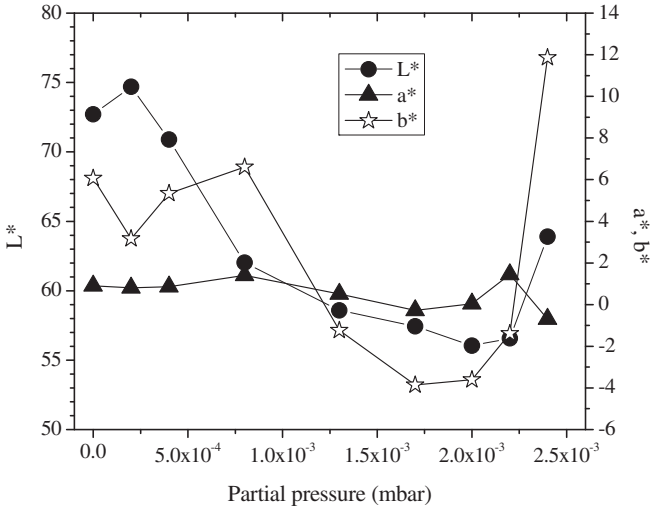

Fig. 7. Evolution of the L*, a*, b* parameters of the TaN_xO_y films as a function of partial pressure during deposition.

From the transmittance spectra of the transparent films and applying the Swanpoel method [24], the refractive index and absorption coefficient (Fig. 6b) of these samples was obtained. An adequate result for the sample $TaN_{0.41}O_{0.91}$, produced with a partial pressure of 2.0×10^{-3} mbar, could not be found. However, the average refractive index of this particular sample was the highest of all the transparent films. This seems to indicate that the optical density of these tantalum oxynitride coatings decreases with increasing partial pressure of the reactive gases during deposition. Such result is justified with the increase of the O content and, as consequence, better conditions to produce the tantalum oxide phase (Ta_2O_5).

Keeping in mind that there might be certain decorative applications for these types of thin solid films, which require certain colours, colour measurements were done, resulting in the L*, a*, b* parameter values. These colour coordinates are plotted as a function of the partial pressure in Fig. 7.

The variation of the lightness (L*), follows, in general, the change in the reflectance, as expected. Therefore, the more reflective surfaces exhibit higher lightness. In general, within zones 1, 2 and T, the lightness decreases with the increase of the non-metal content in the films. For the films of zone 3 it is noticed that the lightness increases with the increase of the partial pressure. This effect is probably caused by the transparency of the films. The L* coordinate of these set of samples is strongly affected by the Si substrate.

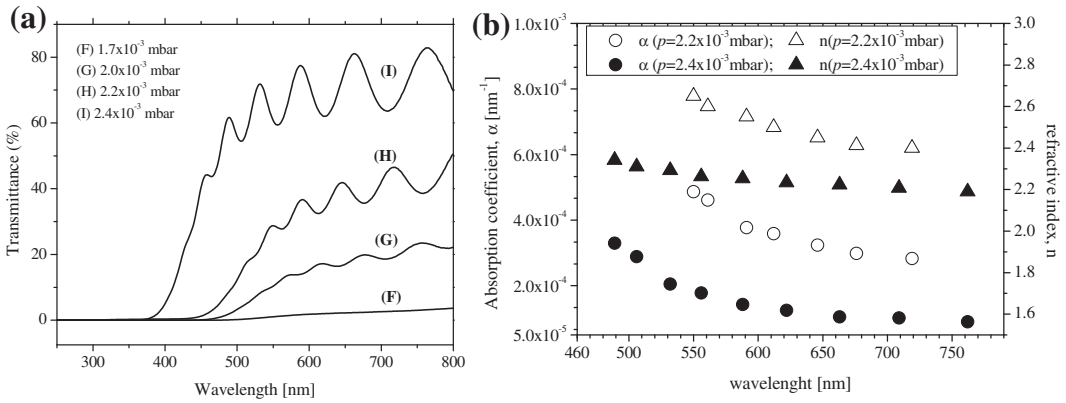

Fig. 6. Transmittance spectra (a) and refractive index and absorption coefficient (b), as function of the wavelength of the incident radiation for the samples that exhibit an interference-like behaviour of the reflectance spectra.

This is also true for the chromaticity coordinates (a* and b*). The L*, a* and b* coordinates of transparent films do not provide a real information of the colour of these films, because they are transparent to the visible light.

For the films grown with lower partial pressures, it is noticed that a* is almost constant (between 0 and 2), but the b* coordinate suffers significant variations. These variations may be correlated with the compositional zones described above. In the films of zone 1, the b* parameter value decreases from ~6.1 to ~3.2 with the increase of N and O content, but when passing to the zone 2 films, an inversion of that tendency occurs, probably due to the change from the β-Ta structure to the fcc Ta(N,O) structure. These two films exhibit b* values between ~5.3 and ~6.6. By increasing the partial pressure, zone T is reached, and a strong decrease of the b* coordinate is clearly observed with a shifting to negative values.

For the films of zones 1 to T, when the non-metal concentration increases, the perceived colour of the films, at daylight, varies from dark grey to brownish grey. Finally, the films of zone 3, register an increase of the b* factor, but as it was referred previously, these films are transparent and the effect of the substrate becomes significant.

3.4. Tribological characterization

In order to assess the tribological behaviour of the TaO_xN_y films, a series of measurements on a reciprocating tribometer was carried out. The duration of the tribo-tests depended on each particular thin film. The experiments were stopped when the evolution of the kinetic friction coefficient (μ_k) with the sliding distance reached a plateau. This plateau corresponds to the friction coefficient of the high-speed steel substrate, sliding against the Si_3N_4 balls. Therefore, reaching this plateau implies a complete removal of the thin film and consequently, the end of the test. Fig. 8 represents the tribological results of the steady-state kinetic friction coefficient as a function of the partial pressure of the reactive gases of the grown films. For comparison, the friction coefficient, in the steady-state regime, of the high-speed steel substrate (AISI M2) against Si_3N_4, is also depicted.

As it is readily seen from the graph, the kinetic friction coefficient values are significantly lower than the one indicated for the substrate material (High-speed steel AISI M2).

The second evidence is that also in terms of the tribological behaviour, the performance of the coatings seems to be correlated with the compositional zones. The TaN_xO_y films that exhibited the highest friction coefficient constitute the last film of zone 1 and those belonging to zone 2. They correspond to the ones having the lowest O content. In the case of zone 2 films, with a fcc Ta(N,O) structure, and among all TaN_xO_y deposited films, these were the ones that exhibited the highest degree of crystallinity. The lowest friction coefficient was obtained for a film belonging to zone T, while the films with the highest O content (zone 3) evidence an increase of the friction coefficient with increasing partial pressure of the reactive gases. Such a trend is probably related to an increase of the coatings' roughness.

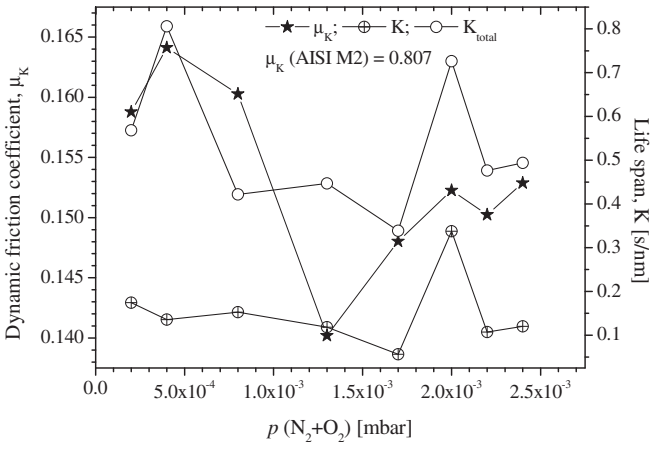

Fig. 8. Friction coefficient values of TaN_xO_y films sliding against Si_3N_4, and their life span as a function of the partial pressure of the reactive gases.

In order to give an estimate of the films' wear resistance, a method based on the evolution of the friction coefficient as function of time was used. As such, the duration (t_1) between the start of the sliding experiment and the precise moments when the first irregularity occurs, which might be due to the first crack, delamination or other destructive event, was recorded. Moreover, the period (t_2) corresponding to the beginning of the test and the precise moment when the friction coefficient reaches the plateau, typical of the substrate's friction level, was also recorded. To eliminate other variables, these two values (t_1 and t_2) were divided by the thickness of the film. Accordingly, using duration t_1, was obtained the lifespan of the film (K), and, using duration t_2, was obtained the total lifespan of the film (K_{total}). The results are plotted as a function of partial pressure in Fig. 8. These values allow the comparison of the wear resistance of each particular coating.

As can be seen, the best wear resistance was obtained for a partial pressure of 4×10^{-4} mbar, corresponding to the $TaN_{0.27}O_{0.20}$ film. It is in fact the first film that belongs to zone 2, and evidences the fcc Ta(N,O) structure. The other film showing a close result corresponds to the one produced with 2×10^{-3} mbar, i.e. $TaN_{0.41}O_{0.91}$, being the first that evidences the interference-like behaviour, as referred previously.

A direct comparison of the normalized life span of the films with the friction coefficient (Fig. 8) is not possible however. It seems though that a general tendency for the films with higher friction coefficients to exhibit better wear resistance exists. The life span decreases with the increase of non-metal content of the nitride-like coatings (produced with lower partial pressure), but increases again after the transition zone coatings, when the O content of the films is higher.

4. Conclusions

TaN_xO_y thin films were produced by dc magnetron sputtering, by varying the reactive gases partial pressure. The set of produced films may be divided in four distinct compositional/structural zones:

Zone 1 ($p(N_2 + O_2) < 2 \times 10^{-4}$ mbar; (N + O)/Ta < 0.1): Metallic films that might be considered as tantalum, with a certain degree of oxygen and nitrogen, due to the partial pressure of the reactive gases during the deposition process.

Zone 2 (2×10^{-4} mbar $< p(N_2 + O_2) < 8 \times 10^{-4}$ mbar; $0.1 < (N + O)/Ta \leq 1$): For the films of this zone, the N/Ta and O/Ta atomic ratios increase with increasing partial pressure of reactive gases, but N/Ta is always higher than O/Ta. The films exhibit a fcc Ta(O,N) structure;

Zone T (8×10^{-4} mbar $< p(N_2 + O_2) < 1.3 \times 10^{-3}$ mbar; $(N + O)/Ta \approx 1$): Films with stable non-metal to metal atomic ratio (close to one) with a slight increase of O content and a slight decrease of the N content, when the partial pressure of the reactive gases, during deposition, increases. This zone corresponds to a transition between the nitride-like samples, produced with lower reactive gas partial pressure (zone 2), and the oxide-like samples (zone 3). The films exhibit a tendency to amorphization;

Zone 3 ($p(N_2 + O_2) > 1.3 \times 10^{-3}$ mbar; (N + O)/Ta > 1): In these films the non-metal to tantalum ratio increases progressively until ~1.6, with a consistent decrease of N concentration and an increase of O concentration. The films are transparent and the refraction index, in the visible region, is higher than 2.2. The optical density of

these coatings decreases with the increase of the non-metal concentration.

The produced tantalum oxynitride coatings exhibit low compressive residual stress, lower than −1 GPa, excepting for the case of one of the samples, which exhibited a tensile stress of around 250 MPa.

The kinetic friction coefficient of the coatings, against a Si_3N_4 ball, is relatively low ($\mu_K < 0.16$). The life span of the nitride-like films shows a tendency to decrease with increasing non-metal content, but for non-metal concentrations higher than those of the transition zone (near stoichiometry), the life span shows a tendency to increase.

Future work concerning this set of coatings will focus on the structural characterization using Raman spectroscopy, but also on the study of the electrical properties and the photo-catalytic behaviour.

Acknowledgements

This paper is supported by the Sectoral Operation Programme Human Resources Development (SOP HRD), ID76945 financed from the European Social Fund and by the Romanian Government.

This work was supported by FEDER through the COMPETE Program and by the Portuguese Foundation for Science and Technology (FCT) in the framework of the Strategic Project PEST-C/FIS/UI607/2011.

References

[1] Barbosa J, Cunha L, Rebouta L, Moura C, Vaz F, Carvalho S, et al. Thin Solid Films 2006;494:201.
[2] Chappé Jean-Marie, Martin Nicolas, Lintymer Jan, Sthal Fabrice, Terwagne Guy, Takadoum Jamal. Applied Surface Science 2007;253:5312.
[3] Braic M, Balaceanu M, Vladescu A, Kiss A, Braic V, Epurescu G, et al. Applied Surface Science 2007;253:8210.
[4] Balaceanu M, Braic V, Braic M, Kiss A, Zoita CN, Vladescu A, et al. Surface & Coatings Technology 2008;202:2384.
[5] Ferreira SC, Ariza E, Rocha LA, Gomes JR, Carvalho P, Vaz F, et al. Surface & Coatings Technology 2006;200:6634.
[6] Huang Jia-Hong, Tsai Zhang-En, Yu Ge-Ping. Surface & Coatings Technology 2008;202:4992.
[7] Ariza E, Rocha LA, Vaz F, Cunha L, Ferreira SC, Carvalho P, et al. Thin Solid Films 2004;469–470:274.
[8] Laurikaitis M, Dudonis J, Milčius D. Thin Solid Films 2008;516:1549.
[9] Westergard R, Bromark M, Larsson M, Hedenqvist P, Hogmark S. Surface and Coatings Technology 1997;97:779.
[10] Kim Deok-kee, Lee Heon, Kim Donghwan, Keun Kim Young. Journal of Crystal Growth 2005;283:404.
[11] Duy Cuong Nguyen, Kim Dong-Jin, Kang Byoung-Don, Yoon Soon-Gil. Materials Science and Engineering B 2006;135:162.
[12] Lu YM, Weng RJ, Hwang WS, Yang YS. Thin Solid Films 2001;398–399:356.
[13] Jagadeesh Kumar K, Ravi Chandra Raju N, Subrahmanyam A. Surface & Coatings Technology 2011;205:261.
[14] Zhou YM, Xie Z, Xiao HN, Hu PF, He J. Applied Surface Science 2011;258:1699.
[15] Zhou YM, Xie Z, Xiao HN, Hu PF, He J. Vacuum 2009;83:286.
[16] Yang WM, Liu YW, Zhang Q, Leng YX, Zhou HF, Yang P, et al. Surface & Coatings Technology 2007;201:8062.
[17] McNamara Karrina, Tofail Syed AM, Conroy Derek, Butler James, Gandhi Abbasi A, Redington Wynette. Nuclear Instruments and Methods in Physics Research B 2012;284:49.
[18] Barradas NP, Jeynes C, Harry MA. RBS/simulated annealing analysis of iron-cobalt silicides. Nuclear Instruments and Methods in Physics Research B 1998;136:1163.
[19] Stoney GG. Proceedings of the Royal Society (London) A 1909;82:172.
[20] Berg S, Nyberg T. Thin Solid Films 2005;476:227.
[21] Lange's handbook of chemistry. 16th ed., McGraw-Hill; page 1:274.
[22] Garg SP, Krishnamurthy N, Awasthi A, Venkatraman M. Journal of Phase Equilibria 1996;17(1).
[23] Cunha L, Vaz F, Moura C, Rebouta L, Carvalho P, Alves E, et al. Surface & Coatings Technology 2006;200:2917–22.
[24] Swanepoel R. Journal of Physics E: Scietific Instruments 1983;18:1214.